

Dynamics of pulsed gas filling of an extended cylindrical tube

© A.V. Arzhannikov,¹ D.A. Samtsov,¹ S.L. Sinitsky,¹ D.A. Starostenko,¹ M.A. Makarov,¹
A.N. Grigoriev,² N.A. Lubenchenko²

¹Budker Institute of Nuclear Physics, Siberian Branch, Russian Academy of Sciences, Novosibirsk, Russia

²All-Russia Research Institute of Technical Physics, Russian Federal Nuclear Center, Snezhinsk, Chelyabinsk oblast, Russia
e-mail: A.V.Arzhannikov@inp.nsk.su

Received May 12, 2025

Revised June 26, 2025

Accepted July 7, 2025

The problem of fast pulse filling of a vacuum cavity inside a long cylindrical tube with a neutral gas is solved. Computer calculations are performed using the Flow Vision package within the Navier–Stokes and KES (k- τ model) models. The first section of the article formulates the requirements for a system of pulse filling of such a tube with gas. Then, the calculation procedure for the filling process is briefly described. A picture of spatio-temporal dynamics of hydrogen flows counter-injected from the ends of the tube to fill it based on the calculation results is presented. The following section presents the results of measurements of the propagation of hydrogen flows along a long tube, which is used to create a plasma cord by a high-voltage discharge at the GOL-PET facility.

Keywords: Navier-Stokes model, k- τ model, pulsed gas injection, gas discharge.

DOI: 10.61011/TP.2026.03.63153.114-25

Introduction

Terahertz (THz) electromagnetic radiation (0.1–10 THz) has an extensive range of scientific, engineering, and practical applications. Examples of its use include plasma heating in thermonuclear research, detection and visualization of hidden objects, study of the spectral characteristics of materials and their processing within the corresponding frequency range, and imaging of fast processes. The spectral interval of 0.3–1 THz remains the least utilized in terms of generation of THz radiation fluxes and recording of the spectral characteristics of objects within the specified frequency range. One approach to solving the problem of generating high-power radiation fluxes within this frequency range is to use the emission from plasma of electromagnetic waves obtained as a result of transformation of an electron plasma wave that is pumped by a high-current relativistic electron beam (REB). Experimental studies in this field have commenced at the GOL-3 facility (Budker Institute of Nuclear Physics, Siberian Branch, Russian Academy of Sciences) in 2010 [1] and are being conducted at present at the GOL-PET facility [2]. Plasma with a minimal charge state of ions is used in these experiments to achieve a high level of plasma oscillations pumped by a beam of relativistic electrons. In view of this, hydrogen is used as the source gas for plasma preparation. Experiments at the GOL-PET facility have demonstrated that the spectral composition of a flux generated in a magnetized plasma column covers the 0.1–0.5 THz frequency range and the maximum of spectral power density is localized near an upper hybrid frequency of 0.15–0.25 THz [3]. The pulse duration is up to 4 μ s, and the total pulse energy

is up to 10 J [4]. The radiation flux emitted from vacuum into the atmosphere has an angular divergence below 10° and propagates over a distance of several meters [5]. The indicated frequency interval in the radiation flux generated at the GOL-PET facility is maintained through the injection of an REB with a current density of 1–2 KA/cm² into a plasma column with an electron concentration of $(5–7) \cdot 10^{14}$ cm⁻³ (see [3,4]). Relying on experience accumulated over decades of experimental research [6–9], we produced this plasma column with the indicated electron concentration by a pulsed high-voltage discharge.

Coupled with theoretical studies into the transformation of upper hybrid plasma oscillations [10–12], the results of experiments at the GOL-PET facility provided a deep understanding of the mechanisms of radiation generation in a beam-plasma system and allowed us to formulate the conditions of transition to the generation of radiation fluxes within the frequency range of 0.5–1 THz [13]. To tap into the specified frequency range, one needs to maintain a plasma concentration at the level of $(5–7) \cdot 10^{15}$ cm⁻³ and a beam current density passing through it on the order of (10–15) KA/cm² with an angular divergence of beam electrons below 0.1 rad. An electron beam satisfying these requirements may be obtained at the linear induction accelerator (LIA) [14] constructed in collaboration between the Budker Institute of Nuclear Physics and the All-Russia Research Institute of Technical Physics. The design of a beam-plasma generator (LIA-PET) utilizing this beam was proposed in [13]. The possibility of compressing the cross section of the LIA beam to the specified current density has already been verified [15]. One of the obstacles to

implementation of the LIA-PET project is that electron emission in the accelerating diode of the linear induction accelerator proceeds from the heated cathode surface, which should be protected from even the slightest influences of residual gases in the high-vacuum accelerator volume. This is the reason why the formation of a plasma cord with the above plasma concentration requires special approaches to filling the gas-discharge gap with gas. It should be filled within a minimum time interval and in such a way that gas entering through fast pulse valves would not reach the accelerator diode. The present study is focused on finding a solution to the problem of rapid filling of the discharge gap, which is an extended tube made of a dielectric material, with hydrogen.

Generally speaking, the engineering task of filling a certain spatial region in a vacuum chamber with gas arises quite often in experiments in beam and plasma physics. An example here is provided by study [16], where the results of experiments with various gas targets used in a point plasma source based on a discharge in a non-uniform gas flow were reported. However, the problem of filling a specific region of space with gas by pulsed injection is rather hard to analyze theoretically [17–20]. In this regard, the problem of pulsed filling of an extended tube, where vacuum was maintained before the gas injection, with gas is defined largely by its geometry.

In the present study, we consider the problem of rapid pulsed filling of a vacuum volume within an extended cylindrical tube with neutral gas. This problem was solved in a specific geometry that is suitable for initiating a high-voltage discharge for the production of a plasma cord with parameters appropriate for injecting an REB with a current density on the order of 10 KA/cm^2 into it. The aim of these calculations is to find the optimal conditions for gas injection into the tube through pulse valves in order to ensure the required uniformity of gas concentration distribution along the length and cross section of the tube. A brief description of the geometry of the pulsed high-voltage discharge system is provided in Section 1. The requirements for the system of pulsed gas supply into a discharge gap are also formulated there. The dynamics of filling a vacuum cavity inside a long quartz tube with gas are examined in Section 2 via computer modeling of the process of propagation of gas flows in the FlowVision package within the Navier–Stokes model. Section 3 presents the results of measurements of the propagation of hydrogen flows along an extended vacuum tube in the high-voltage discharge former of the GOL-PET facility implemented in such a way as to meet the requirements for the plasma cord of the future LIA-PET facility. The obtained data on patterns of pulsed filling of a vacuum cavity inside a tube with neutral gas in preparation for a high-voltage discharge producing a plasma cord with the required parameters are summarized in Conclusion.

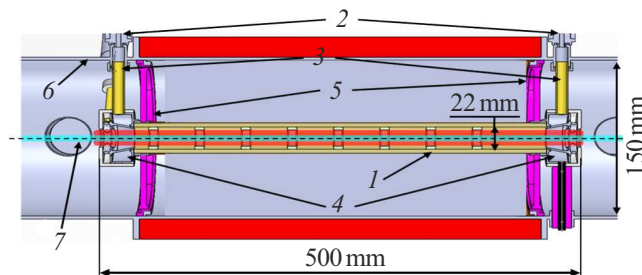


Figure 1. Schematic diagram of the gas-discharge chamber of the LIA-PET beam-plasma generator. 1 — Quartz tube confining the region of plasma discharge formation; 2 — fast pulse valves ensuring gas supply to the vacuum volume; 3 — tubes for gas supply from the pulse valves to nozzles located at the ends of the quartz tube; 4 — two coaxial nozzles for hydrogen injection into the quartz tube; 5 — diaphragms securing the quartz tube in the vacuum chamber; 6 — cylindrical steel vacuum chamber; and 7 — region of REB propagation in the experiment.

1. Geometry of the space for pulsed gas filling

Experiments on the generation of THz radiation fluxes at the LIA-PET accelerator complex will require the formation of a thin extended plasma cord with parameters sufficient for exciting upper hybrid plasma waves during the passage of a beam of relativistic electrons. The geometry of the high-voltage discharge gap needed for such a plasma cord is presented in Fig. 1. A current density in the discharge gap at the level of 5 KA/cm^2 is needed to achieve the required plasma electron density ($\sim 7 \cdot 10^{15} \text{ cm}^{-3}$) through hydrogen ionization by a high-voltage discharge. A quartz tube 22 mm in diameter with dielectric rings with a diameter of 16 mm positioned inside it (see Fig. 1) was chosen as a means to confine the gas cloud for a high-voltage discharge.

A system for forming this cylindrical gas cloud by pulsed injection of hydrogen into the quartz tube through slot nozzles installed at its ends was considered.

This system of rapid pulsed production of a thin cylindrical cloud has three main elements. The key element is a Festo pulse solenoid valve with the required pressure of injection gas maintained at its input. Gas injected through the pulse valve propagates to the slot nozzle at the end of the quartz tube via a metal tube with an internal diameter of 6 mm and an approximate length of 100 mm. This propagation of gas during pulsed operation of valves was modeled in computer calculations.

It should be noted that the use of the LIA as the initial REB source requires maintaining residual vacuum at the level of 10^{-7} Pa (10^{-9} Torr) outside the high-voltage plasma discharge section. Under such conditions, the amount of gas injected through the pulse valves into the vacuum volume needs to be minimized. At the same time, a plasma concentration around $5 \cdot 10^{15} \text{ cm}^{-3}$ should be provided in a plasma cord produced in the quartz tube. The system of pulsed gas injection into the vacuum cavity of the

quartz tube, where a high-voltage discharge produces a plasma cord, must satisfy these (somewhat contradictory) requirements.

The dimensions of the spatial region where a plasma cord is formed are set by the internal diameter of the quartz tube (22 mm) and its length (330 mm). The diameter of a beam of relativistic electrons propagating through this cord should not exceed 12 mm, and the plasma cord diameter, which is set by diaphragms, is 16 mm. Gas flows are injected from both ends of the tube toward each other through axially symmetrical nozzles. Gas is transported from the valves to these nozzles along special tubes with a diameter of 8 mm. Nozzle flows must form a uniform azimuthal distribution of gas. In the discussed geometry of pulsed gas supply to the tube, the gas flow into the remaining space, where high vacuum is maintained by continuous evacuation, should be minimized. It was this geometry of pulsed gas injection that was used in model calculations of filling of an extended quartz high-voltage discharge tube with gas.

2. The process of solving the problem in FlowVision and the results obtained

Model gas dynamics calculations are intended to characterize the dependence of parameters of an extended gas cloud (the characteristic time of filling the tube with gas, the achieved concentration, its uniformity in cross section and length) on geometric dimensions of the pulsed gas supply system and the time for which the gas supply valve stays open (with special attention paid to the dynamics of the process of its opening). In what follows, we detail a calculation with notes taken of the characteristic features of the problem being solved and analysis of the results obtained.

To implement a specific solution to the problem within the chosen approach, a three-dimensional computer model of the spatial region occupied by the plasma section was created first. The purpose of modeling was to characterize the dynamics of temporal variation of the gas density distribution along the length of the gas-discharge tube. The dynamics of gas propagation from the pulse valves through the supply tubes connected to them to the annular slot nozzles at the ends of the gas-discharge quartz tube were monitored in the process of simulation (in Fig. 1, the quartz tube and the supply tubes are denoted by numbers 3 and 6, 7, respectively, while the valves are not shown). The propagation of gas was monitored in particular detail in the quartz gas-discharge tube where a thin plasma cord is to be produced.

The specialized FlowVision package was used for model calculations. These calculations were performed within the Navier–Stokes model. A „step“ model of valve operation with full opening of the valve in an infinitely small period of time and its instantaneous closing was used. The hydrogen consumption within 0.5 ms of the open state of this kind of valve corresponds approximately to the

hydrogen consumption in operation according to the model of linear increase and decline in transmitted flow with a total duration of 1 ms („triangular“ time diagram).

Several series of calculations were carried out in FlowVision in order to determine the characteristic times of filling of the vacuum cavity of the quartz tube with gas. The calculation procedure was typical for a software package of this type. The geometry (in the form of a 3D object) and conditions at the boundaries of the object through which gas flows are introduced and/or ejected were specified first. The initial conditions, which include the gas type (in the present case, hydrogen) and the turbulence model used in calculations, were formulated at this point. The cross sections of spatial regions in which the gas flow parameters of interest to us (concentration, pressure, temperature) need to be tracked were defined next. At specified initial time points, sections of the object boundary were opened, and gas was injected through them into vacuum (this corresponds to opening of the valves located at the inlet of the supply tubes). At a certain subsequent point in time (in our simulations, 0.5 ms), the „wall“ condition was set at the inlet of these tubes: the gas supply was cut off due to instantaneous closing of the valve. Further calculations were carried out without gas supply from external sources.

The FlowVision database was used: hydrogen was treated as a gaseous equilibrium material medium. The following tabular values were taken from this database in the process of calculation: molar mass, thermal conductivity, viscosity, specific heat capacity, and enthalpy; density was determined from the ideal gas equation. The values of pressure and temperature were calculated iteratively to an accuracy of 0.01 % based on the ideal gas equation. The used model of heat transfer in terms of total enthalpy implied a change in temperature during the calculation.

The characteristic flow velocity in the supply tube was $\sim 2\text{--}3\text{ km/s}$, and the Mach number was as high as $M \sim 2.5$. The diameter of the opening in the valve was 1 mm (this was covered by ten grid cells); Reynolds number¹ behind the valve $Re_{valve} \sim 4000$; the diameter of tubes leading to the cylindrical receiver was 8 mm; Reinlet tube ~ 700 ; the quartz tube diameter was 22 mm (18 cells fit into this diameter); and Reynolds number behind the cylindrical receiver $Re_{quartz\ tube} \sim 3\text{--}9$. The minimum and maximum grid pitches were 0.1 and 2.5 mm; the calculation time step was varied: $10^{-10}\text{--}10^{-3}\text{ s}$ (a specific value was chosen automatically by the solver). The calculation was carried out up to time point $t = 3\text{ ms}$. It took approximately one month to perform calculations for one model option.

The K- ϵ turbulence model was used in the first (preliminary) calculations to solve the problem of filling of the gas-discharge tube with hydrogen. It turned out that when flow turbulence is introduced into the description of gas

¹ The Reynolds number was estimated as $Re = \frac{\rho|V|L}{\mu}$, where ρ is the density, $[\text{kg}\cdot\text{m}^{-3}]$; $|V|$ is the velocity modulus, $[\text{m}\cdot\text{s}^{-1}]$; L is the characteristic dimension (the tube size was used in estimates), $[\text{m}]$; and μ is the viscosity (dynamic coefficient of molecular viscosity), $[\text{Pa}\cdot\text{s}]$.

transmission along the tube transferring hydrogen from the valve to the nozzle, the duration of calculations increases significantly, while the length of the time interval needed to fill the quartz tube with hydrogen increases only slightly (by less than 2%). Relying on the results of this series of preliminary calculations, we neglected turbulence in solving the problem of gas transfer through supply tubes in subsequent series of systematic calculations of the dynamics of filling the quartz gas-discharge tube. The Navier–Stokes equation was solved in this formulation of the problem without additions to the viscous force. It should be noted that this formulation could lead to overestimation of temperature in the region of space where flows propagating from the nozzles at the ends of the gas-discharge tube meet in its middle part (lengthwise). In addition to the Navier–Stokes equation, the model of heat transfer in terms of total enthalpy (the energy conservation equation in terms of total enthalpy) was used in the solution.

The numerical algorithm implemented in FlowVision is actually independent of the local Mach number and, given a correct set of parameters, allows us to calculate flows with subsonic, transonic, supersonic, and hypersonic velocities.

The maximum hydrogen velocity in the solver was set to 4000 m/s, which corresponds to the maximum thermal velocity of hydrogen molecules in their velocity distribution function. This limit was necessitated by the assumption of instantaneous valve opening used in calculations² on account of the resulting steep temperature gradient over the entire calculated volume of space, which may also be attributed to invalid treatment of the effects associated with gas motion and compression.

More than 1.2 million cells were contained in the calculated region of space. Figure 2, *a*, which presents the computational grid for the supply tube and nozzle volumes, illustrates the arrangement of cells. With this grid used, a second-order implicit difference scheme with Courant–Friedrichs–Lewy number $CFL = 1$ was implemented.

The initial conditions included the pressure on the inlet valves (10^5 Pa), a constant initial temperature (297 K), the initial pressure in the chamber (1 Pa), and the gas temperature (297 K) in the calculation region at the initial moment of time. It should be noted outright in this context that a limit on the initial pressure of residual gas in the vacuum chamber at a level of at least 1 Pa was found to be necessary for correct application of FlowVision in calculations. This restriction is associated with violation of applicability conditions of the Navier–Stokes equations used in the program. The applicability criterion is Knudsen number K_n , which is defined as the ratio of mean free path

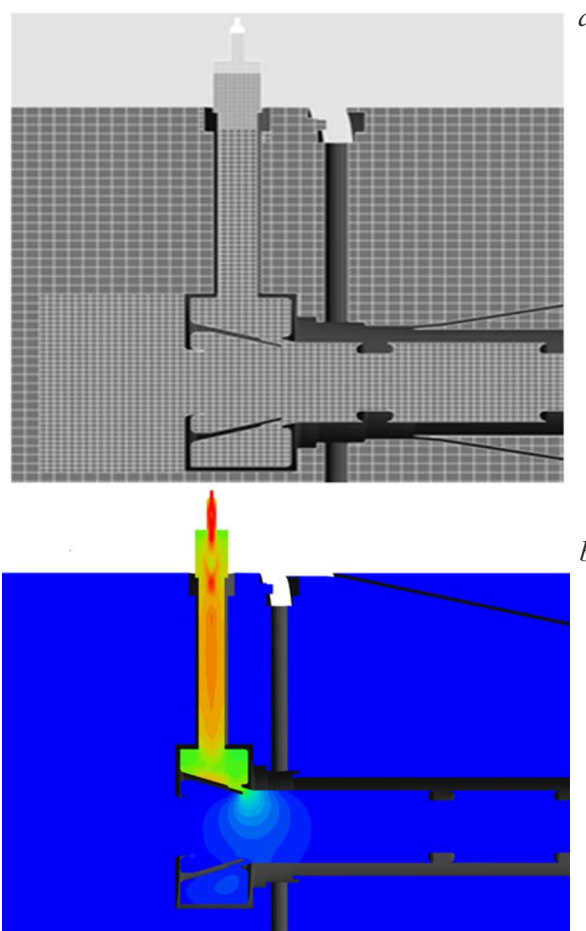


Figure 2. Computational grid covering the supply tube volume, the nozzle, the gas-discharge tube, and the surrounding space (*a*) and calculated distribution of hydrogen concentration at time $t = 0.8$ ms from the moment valve opening is initiated (*b*).

of particles $\langle l \rangle$ to characteristic dimension L of the system:

$$K_n = \langle l \rangle / L.$$

The Navier–Stokes equations may be used if condition $K_n \ll 1$ is satisfied. Having estimated the mean free path for hydrogen molecules (i.e., the molecules of interest to us) based on the kinetic theory of gases, we obtain

$$\langle l \rangle = k_b T \sqrt{2\pi} d^2 p \approx 10m.$$

With characteristic dimension $L = 22$ mm of the system (tube diameter) and residual pressure $p = 10^3$ Pa, we find that $K_n = 4.6 \cdot 10^2$. Thus, the parameters of the gaseous medium under consideration lie far from the applicability range of the Navier–Stokes equations. At the same time, the Knudsen number estimate at residual pressure $p = 1$ Pa is $K_n = 4.6 \cdot 10^{-1}$, which means that the conditions of the problem correspond to the description of conditions in the transition region between a continuous medium and a free molecular flow.

Thus, the problem was solved with the pressure at the valve inlets set equal to the atmospheric one; according to

² Additional calculations, which are presently being carried out, reveal that when a realistic model of the valve opening process, which ensures a pressure rise without jumps, is specified, the outflow velocity does not exceed 3.2 km/s; i.e., the Mach number reaches $M \sim 2.5$ – 2.6 (the speed of sound in hydrogen is $v_s \sim 1290$ m/s at 1 atm and $v_s \sim 1200$ m/s at 1 Pa).

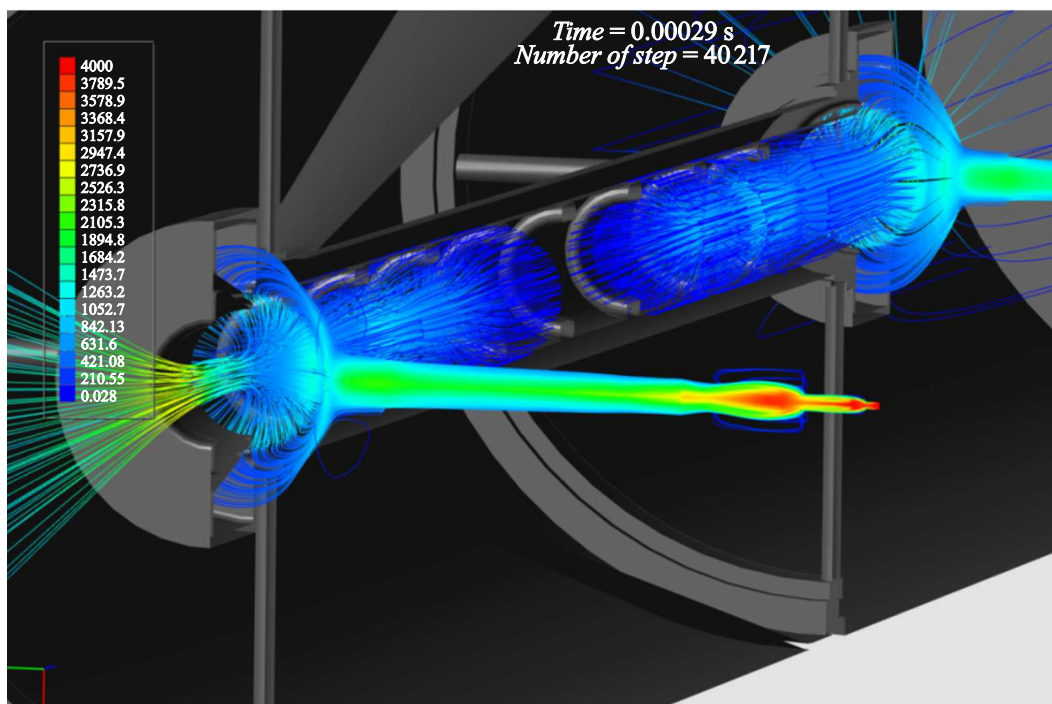


Figure 3. Visualization of flow velocity lines, [m/s], for hydrogen in the gas-discharge chamber of the LIA-PET beam-plasma generator.

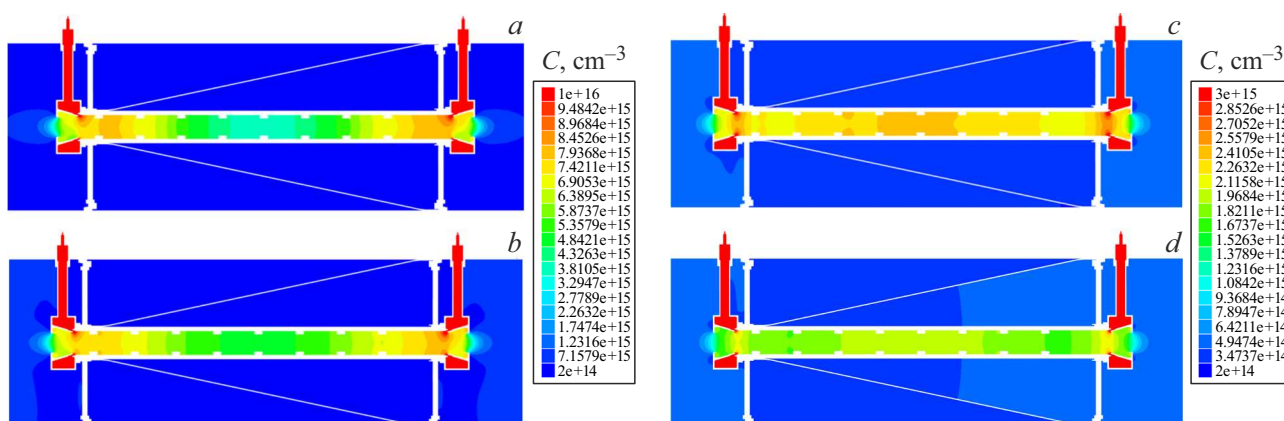


Figure 4. Distributions of hydrogen concentration (axial section) at different points in time: *a* — $t = 0.92$ ms; *b* — $t = 1.12$ ms, $C_{t,m} \sim 2.5 \cdot 10^{16} \text{ cm}^{-3}$; *c* — $t = 1.81$ ms; *d* — $t = 2.20$ ms, $C_{t,m} \sim 1.6 \cdot 10^{16} \text{ cm}^{-3}$.

the above analysis, the problem of gas distribution within the volume could be solved correctly down to a minimum pressure in it on the order of 1 Pa. In regions with lower pressure levels, the solution provided by the specialized FlowVision program may be incorrect.

Note that a series of calculations performed in order to obtain at least an approximate dependence of the tube filling time on the initial residual gas pressure in requires a large amount of computer time. This is the reason why this problem is the subject of a separate series of calculations with a significant expenditure of computer time. However, with the dependence of the gas flow velocity on the pressure gradient taken into account, it is fair to assume that an order-of-magnitude reduction in initial pressure in the quartz tube

translates into just a several percent increase in time needed to fill it to the required hydrogen distribution.

First of all, it was determined in modeling how the diameter and length of the tube along which gas is supplied from the valve outlet to the nozzle affect the gas flow through the nozzle into the high-voltage discharge region in the quartz tube. The results of these calculations were used to set the proper diameter of the supply tube. Taking into account the conditions of practical implementation of the pulsed gas injection system in upcoming experiments, we chose a supply tube diameter of 8 mm. The results of calculations for the internal cavity of the quartz tube filled with a supply tube of this diameter are presented in Figs. 3–7.

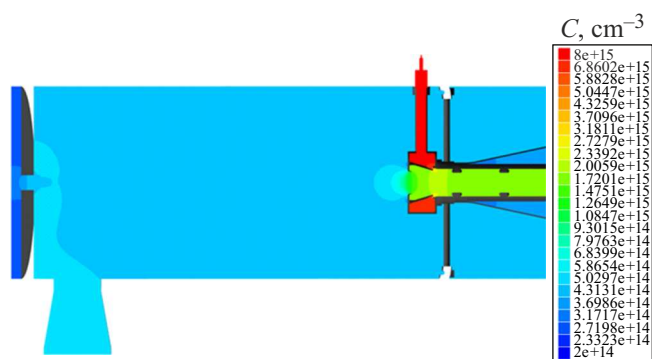


Figure 5. Distribution of hydrogen concentration in the buffer volume between the gas-discharge tube and the accelerator beam inlet at time point $t = 2.3$ ms.

The distribution of hydrogen concentration at time point $t = 0.8$ ms (time is counted from the moment of instantaneous opening of the valve) is shown in Fig. 2, *b*. It bears reminding that the valve stays open for 0.5 ms.

The results of calculation with visualization of flow velocity lines for hydrogen propagating in the plasma discharge formation system of the LIA-PET facility are shown in Fig. 3.

The obtained data on the dynamics of filling the internal cavity of the quartz gas-discharge tube with hydrogen are presented in Fig. 4. The upper limit of hydrogen concentration C indicated on the right does not represent in full the maximum concentration in the local region. In connection with this, the maximum values of hydrogen concentration in supply tube $C + t.m$ are also indicated in captions.

The presented plots make it evident that the gas-discharge tube gets filled with hydrogen entering through axially symmetric nozzles located at both ends of the tube within a time interval on the order of 0.6 ms. Therefore, the characteristic time scale of hydrogen propagation along the length of the gas-discharge tube is approximately 1 ms.

It is important to note that the contact of hydrogen with the heated cathode surface in the LIA accelerator diode, which produces the beam injected into the plasma cord, was prevented through the use of a large buffer volume with a diameter of 10 cm and a length of 0.3 m. The outflow of hydrogen from this volume toward the accelerator diode was limited by a diaphragm with an opening 16 mm in diameter. The outflow of hydrogen from the buffer volume through this diaphragm was characterized within the model of free outflow of gas with expansion into vacuum.

The distribution of hydrogen concentration at time point $t = 2.3$ ms outside the gas-discharge tube in the vicinity of

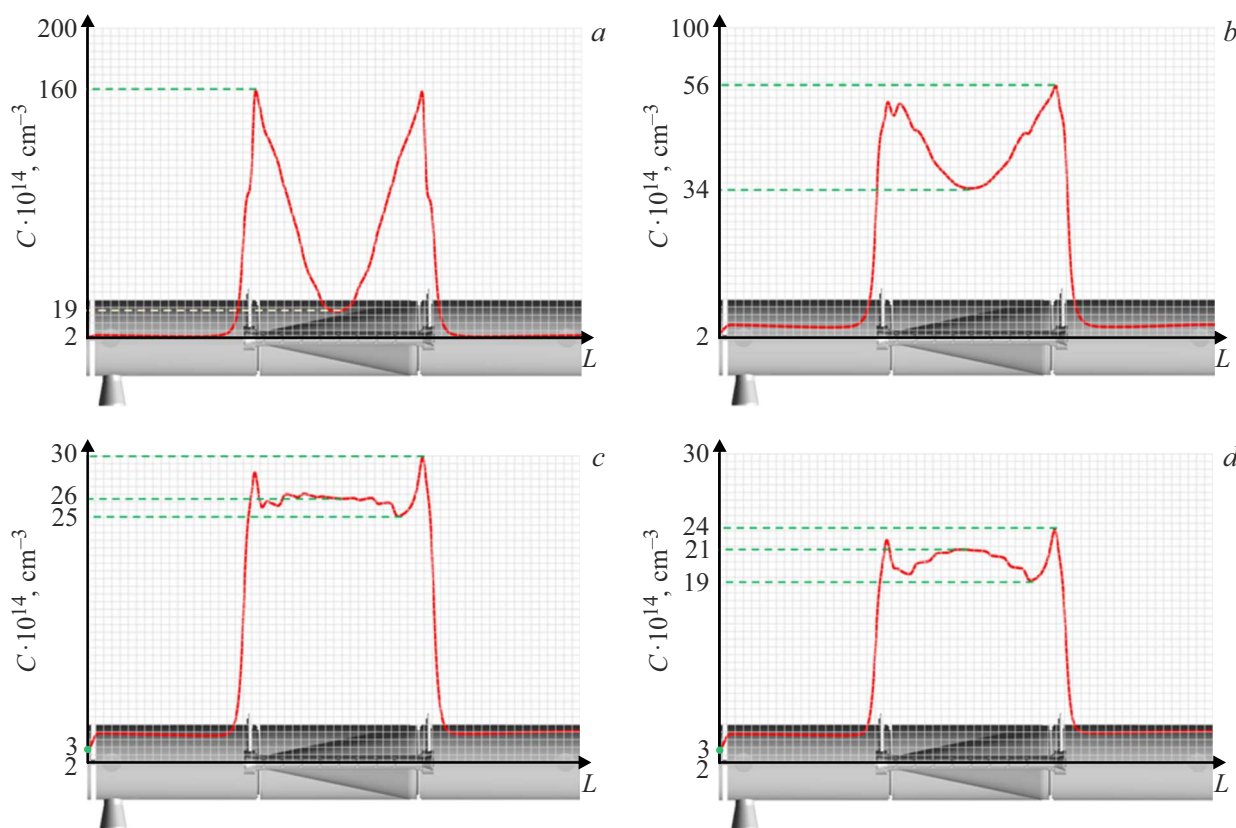


Figure 6. Distributions of the maximum hydrogen concentration (axial section) at different points in time, t , ms: *a* — 0.52, *b* — 0.112, *c* — 1.61, *d* — 2.01.

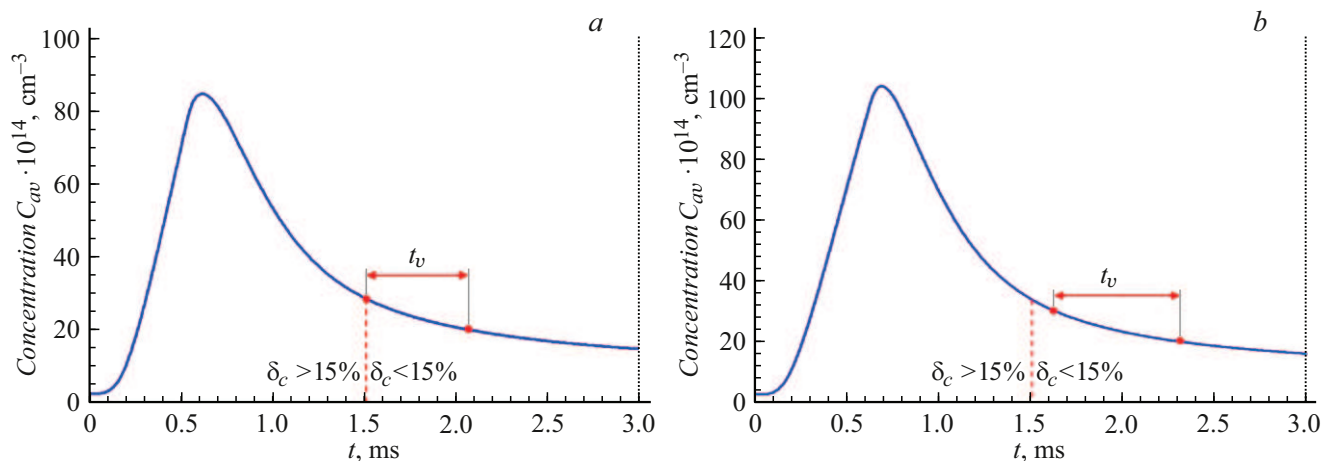


Figure 7. Dependences of volume-averaged concentration C_{av} of hydrogen in the tube on time: *a* — valve open for 0.5 ms; *b* — valve open for 0.6 ms. The dashed vertical line corresponds to the transition from a non-uniform concentration distribution ($\delta_c > 15\%$) to a uniform one ($\delta_c < 15\%$); t_v is the time interval within which the average concentration value in the central region of the tube remains within the $C_{av} \approx (2-3) \cdot 10^{15} \text{ cm}^{-3}$ range.

the opening for injection of the electron beam into the end of the plasma cord is presented in Fig. 5. This opening is shown on the axis of symmetry at the left edge of the image. It can be seen that the hydrogen flow coming from the valve expands within a large buffer volume, producing a low density level behind the opening that is acceptable for injection of the electron beam from the accelerator.

At the same time, the hydrogen concentration inside the gas-discharge tube is sufficient for a high-voltage discharge. Figure 6 shows the distribution of hydrogen concentration along the length of the gas-discharge tube in the axial section for a series of successive time points.

These plots make it clear that the hydrogen concentration distribution along the length of the gas-discharge tube reaches an acceptable level of uniformity over a time scale of 1.5–2 ms (counted from the moment when the opening of hydrogen valves is initiated). The time dependence of hydrogen concentration C_{av} averaged over the volume of this tube is shown in Fig. 7, *a*. The dashed vertical line serves as a boundary between two variants of tube filling with gas. The first is non-uniform filling: relative deviation δ_c of concentration from its average value satisfies condition $\delta_c > 15\%$. The second variant is uniform filling with $\delta_c < 15\%$.

The required relative deviation $\delta_c = \pm 15\%$ from the volume-average concentration value $C_{av} = 2.0-2.5 \cdot 10^{15} \text{ cm}^{-3}$ is established within 1.65 ms ($t = 0$ is the moment when valve opening is initiated). A uniform distribution of hydrogen concentration is maintained for $t_v = 0.45$ ms (through to $t = 2.1$ ms). At subsequent points in time, the hydrogen concentration becomes lower than $C_{av} = 2.0 \cdot 10^{15} \text{ cm}^{-3}$, which is unacceptable in the context of generation of plasma with the required density via a high-voltage discharge. Figure 7, *b* presents the result obtained when the duration of the open

valve state was increased from 0.5 to 0.6 ms. Comparing Figs. 7, *a* and *b*, one sees that the shape of concentration dependence on time $C_{av} = f(t)$ is reproduced well when the duration of the open valve state is varied slightly. It is also evident that hydrogen concentration C_{av} in the gas-discharge tube at ~ 2 ms is at the level of $2 \cdot 10^{15} \text{ cm}^{-3}$ with fine uniformity of distribution over the volume of the gas cord, which is necessary for experiments on beam injection into the formed plasma cord. It should be noted that adjustment of the duration of the open valve state may be used alongside with a shift of point t_w of initiation of the high-voltage discharge and, accordingly, of the time point of injection of the electron beam into plasma for the purpose of varying the required plasma density in experiments.

Thus, the following conclusions may be formulated based on the results of model calculations. The regime of hydrogen supply through the supply tubes to the nozzles has little effect on the distribution of gas concentration in the quartz gas-discharge tube. The presented distributions of hydrogen concentration along the length of the discharge tube reveal that a reduced hydrogen concentration is established precisely in its middle region, where counter-flows of gas injected from the nozzles collide with each other. The average and maximum values of hydrogen concentration in this gas-discharge tube are determined largely by the total volume of hydrogen injected via the supply tubes from the pulse valves. In the presented calculation variants, the hydrogen concentration averaged over the cord cross section at the moment of valve closing falls within the required range of $(2-3) \cdot 10^{15} \text{ cm}^{-3}$.

A uniform distribution of gas concentration persists within the time interval of 560–680 μs . This duration ($\sim 120 \mu\text{s}$) is entirely sufficient to produce a plasma cord, since the current rise time in a high-voltage discharge, which provides the required degree of gas ionization, is

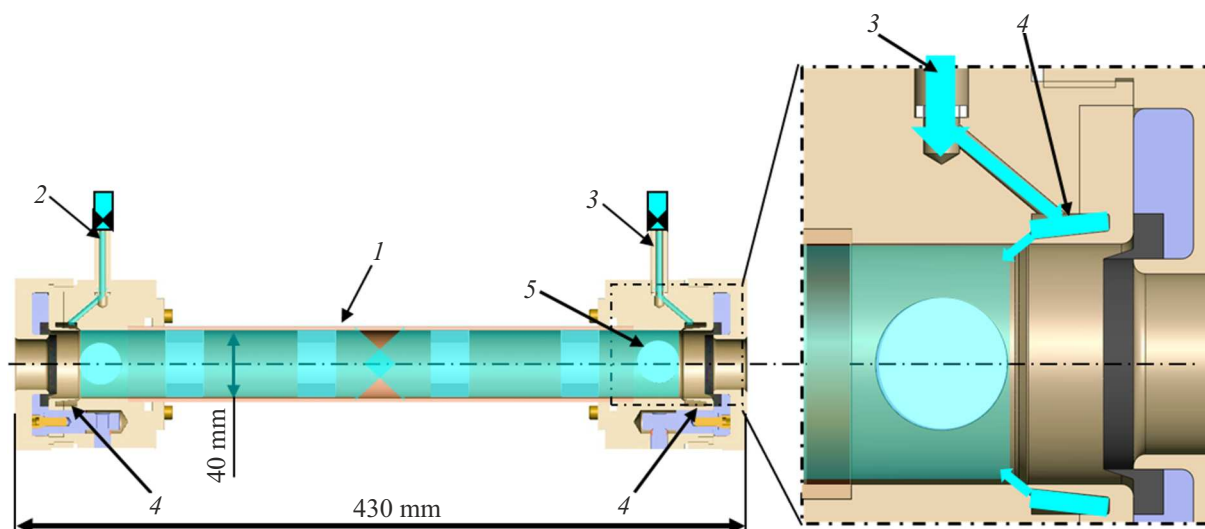


Figure 8. Schematic diagram of the system of plasma cord formation by a high-voltage discharge at the GOL-PET facility. 1 — Quartz tube 40 mm in diameter with \varnothing 36 mm annular diaphragms limiting the gas cord diameter; 2 — valve with a tube for pulsed hydrogen supply to the first nozzle; 3 — valve with a tube for pulsed hydrogen supply to the second nozzle; 4 — two coaxial slot nozzles for injecting hydrogen from the valves into the quartz tube; and 5 — window through which the PMI-10-2 measuring lamp is connected.

2.5–3 μ s. It is arguable that there should be no difficulty in implementing gas ionization in an experiment where a uniform distribution of gas density persists for such a long time. It is necessary in this case to choose the right moment of discharge ignition relative to the time interval within which the valves stay open. It should be noted that a plasma cord produced by a high-voltage discharge in an experiment persists for several tens of microseconds.

3. Results of measurements of the time of hydrogen passage through the tube

The reliability of the above modeling results for the process of filling of an extended tube with hydrogen is confirmed by experiments in this field that have been conducted earlier at the GOL-PET facility. The modernization of this facility for such experiments was discussed in [21], where data on the systems for gas injection and formation of a high-voltage discharge current were presented. Here, we provide only a brief account of the results of measurements for hydrogen flows propagating through the tube. The diagram for measuring the propagation of hydrogen supplied via FESTO MH-1 pulse valves through the gas-discharge tube at the GOL-PET facility is shown in Fig. 8. Gas was supplied through long metal tubes from the pulse valves to the axially symmetric slot nozzles located at the ends of the gas-discharge quartz tube. A detailed view of the connection between the metal tube and the nozzle is presented on the right side of Fig. 8.

The geometry of experiments conducted at the GOL-PET facility differs from the geometry of model calculations that characterize the filling of the tube at the future LIA-PET facility. The operating GOL-PET facility has a guiding

magnetic field in the vacuum chamber of 4 T, and the pulse valves are therefore positioned at a distance of 50 cm from the chamber axis (i.e., significantly further away than at the LIA-PET facility, where the corresponding distance will be 8 cm with a field induction of 1 T). The time needed for hydrogen to propagate along the quartz tube was determined by recording the process of pressure rise in the vicinity of a PMI-10 measuring lamp, which was located at one of its ends. The pulse valves were actuated at a fixed pressure at their inlet of 2 atm. The process of pressure rise in the vicinity of the measuring lamp was recorded with three types of valve operation dynamics: with hydrogen supplied only through the pulse valve positioned at the other end of the discharge tube (in relation to the measuring lamp), only through the valve located at the end of the tube closest to the measuring lamp, and through both valves simultaneously. The variations of pressure in the vacuum chamber recorded with these three hydrogen supply options in the region where the PMI-10 measuring lamp is located are presented in Fig. 9.

The magnitude of pressure in the local region around the lamp is expressed in relative units. Figure 9, *a* illustrates the dynamics of opening and closing of the valves used in these experiments. Figure 9, *b* shows the complete cycle of pulsed variation of pressure in the vacuum chamber from its rise (when the valves are opened) to the return to the initial high-vacuum state.

The time diagrams presented in Figs. 9, *a*, *b* make it evident that the approximate time of gas propagation from the pulse valves to the slot nozzles located at the ends of the gas-discharge tube is 5 ms. This delay in gas injection into the gas-discharge gap relative to the moment of valve opening is attributable to the large (50 cm) length of tubes

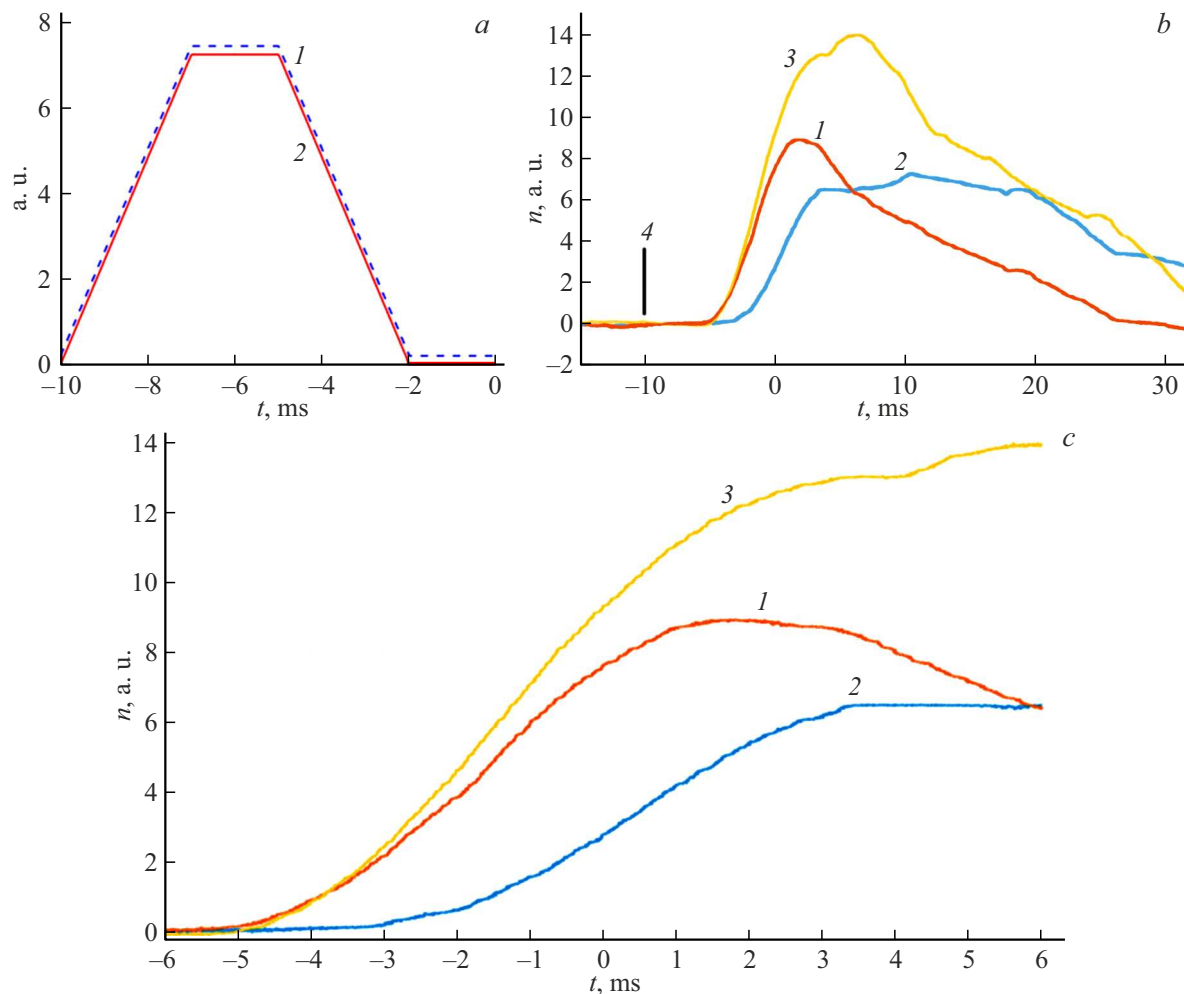


Figure 9. Pressure variations recorded in a local region of the vacuum chamber where the measuring lamp is located: *a* — time diagram of hydrogen injection through valves *1* and *2*; *b* — temporal variation of signals from the lamp that measures pressure. Signal from the lamp: red line *1* — with the valve closest to it triggered; blue line *2* — with the valve located at the opposite end of the quartz tube triggered; yellow line *3* — with both valves triggered simultaneously. The vertical line in panel (*b*) (denoted by number *4*) indicates the time point when the opening of valves, the dynamics of which are illustrated in panel (*c*), is initiated.

connecting the valves to the nozzles. The time dynamics of signals *1* and *2* in Fig. 9, *c* allow one to determine that the time of passage of a pressure wave from one end of the quartz discharge tube to the other with the given geometry and parameters of the hydrogen supply system to the slot nozzles is approximately 2 ms. This measured value agrees closely with the time of filling of such a tube with hydrogen that was obtained as a result of computer simulations.

Conclusion

Computer modeling of the spatiotemporal dynamics of filling of an extended quartz tube with hydrogen was carried out with a focus on the production of a thin plasma cord (for subsequent generation of terahertz radiation through intense relaxation of a relativistic electron beam in magnetized plasma) in this tube by a high-voltage discharge. This simulation revealed the following.

When an extended (length, 30 cm; diameter, 20 mm) quartz gas-discharge tube is filled with hydrogen supplied from both its ends through coaxial slot nozzles from two pulse valves, it is sufficient to open them for approximately 1 ms to reach a concentration of molecules in the tube at the level of $(2-3) \cdot 10^{15} \text{ cm}^{-3}$ at a pressure on the valves of 1 atm.

As this tube is filled with two counter flows of hydrogen entering through the slot nozzles at both ends, a uniform distribution of hydrogen concentration along the length of the tube is achieved within the time of their mutual lengthwise penetration, which turns out to be at the level of 2 ms. Our experience accumulated in similar numerical calculations suggests that the error of the obtained calculated value of the discharge tube filling time is no higher than 20%.

In turn, experiments on pulsed filling of an extended quartz tube with hydrogen carried out at the GOL-PET

facility revealed that the time of its filling with counter flows from both ends is indeed close to 2–3 ms.

Thus, the results of computer modeling and test experiments demonstrated that high voltage should be applied to the electrodes at the ends of the quartz tube 2–3 ms after the onset of hydrogen outflow from the slot nozzles when a high-current discharge is ignited for the purpose of forming a plasma cord in the tube. The achieved parameter levels are suitable for production of a thin plasma cord for generating terahertz radiation in the process of intense beam-plasma interaction at the LIA-PET facility.

Conflict of interest

The authors declare that they have no conflict of interest.

References

- [1] A.V. Arzhannikov, A.V. Burdakov, P.V. Kalinin, S.A. Kuznetsov, M.A. Makarov, K.I. Mekler, S.V. Polosatkin, V.V. Postupaev, A.F. Rovenskikh, S.L. Sinitsky, V.F. Sklyarov, V.D. Stepanov, Yu.S. Sulyaev, M.K.A. Thumm, L.N. Vyacheslavov. *Vestnik Novosibirsk State University. Series: Phys.*, **5** (4), 44 (2010). DOI: 10.54362/1818-7919-2010-5-4-44-49
- [2] A.V. Arzhannikov, A.V. Burdakov, V.S. Burmasov, I.A. Ivanov, A.A. Kasatov, S.A. Kuznetsov, M.A. Makarov, K.I. Mekler, S.V. Polosatkin, S.S. Popov, V.V. Postupaev, A.F. Rovenskikh, S.L. Sinitsky, V.F. Sklyarov, V.D. Stepanov, I.V. Timofeev, M.K.A. Thumm. *IEEE Transactions on Terahertz Sci. Technol.*, **6** (2), 245 (2016). DOI: 10.1109/TTHZ.2016.2525783
- [3] A.V. Arzhannikov, S.L. Sinitsky, D.A. Samtsov, I.V. Timofeev, E.S. Sandalov, S.S. Popov, M.G. Atlukhanov, M.A. Makarov, P.V. Kalinin, K.N. Kuklin, A.F. Rovenskikh, V.D. Stepanov. *Plasma Phys. Rep.*, **50** (3), 331 (2024). DOI: 10.1134/S1063780X24600051
- [4] A.V. Arzhannikov, S.L. Sinitsky, S.S. Popov, I.V. Timofeev, D.A. Samtsov, E.S. Sandalov, P.V. Kalinin, K.N. Kuklin, M.A. Makarov, A.F. Rovenskikh, V.D. Stepanov, V.V. Annenkov, V.V. Glinsky. *IEEE Transactions Plasma Sci.*, **50** (8), 2348 (2022). DOI: 10.1109/TPS.2022.3183629
- [5] D.A. Samtsov, A.V. Arzhannikov, S.L. Sinitsky, M.A. Makarov, S.A. Kuznetsov, K.N. Kuklin, S.S. Popov, E.S. Sandalov, A.F. Rovenskikh, A.A. Kasatov, V.D. Stepanov, I.A. Ivanov, I.V. Timofeev, V.V. Annenkov, V.V. Glinskiy. *IEEE Transactions Plasma Sci.*, **4**, 9(11), 3371 (2021). DOI: 10.1109/TPS.2021.3108880
- [6] A.V. Arzhannikov, A.V. Burdakov, P.P. Deichuli, V.S. Koidan, V.V. Konyukhov, K.I. Mekler. *Fiz. Plazmy*, **4** (5), 1133 (1978) (in Russian).
- [7] A.V. Burdakov, V.S. Koidan, K.I. Mekler, S.V. Polosatkin, V.V. Postupaev. *Plasma Phys. Rep.*, **40**, 161 (2014). DOI: 10.1134/S1063780X14030039
- [8] A.V. Arzhannikov, A.V. Burdakov, V.S. Burmasov, I.A. Ivanov, S.A. Kuznetsov, K.N. Kuklin, K.I. Mekler, S.V. Polosatkin, V.V. Postupaev, A.F. Rovenskikh, S.L. Sinitsky, V.F. Sklyarov. *Plasma Phys. Rep.*, **41** 863 (2015). DOI: 10.1134/S1063780X1511001X
- [9] A.V. Arzhannikov, I.A. Ivanov, P.V. Kalinin, A.A. Kasatov, M.A. Makarov, K.I. Mekler, A.F. Rovenskikh, D.A. Samtsov, E.S. Sandalov, S.L. Sinitsky. *J. Phys.: Conf. Ser. IOP Publishing*, **1647** (1), 012011 (2020). DOI: 10.1088/1742-6596/1647/1/012011
- [10] A.V. Arzhannikov, I.V. Timofeev. *Plasma Phys. Controlled Fusion*, **54** (10), 105004 (2012). DOI: 10.1088/0741-3335/54/10/105004
- [11] I.V. Timofeev, V.V. Annenkov, A.V. Arzhannikov. *Phys. Plasmas*, **22** (11), 113109 (2015). DOI: 10.1063/1.4935890
- [12] A.V. Arzhannikov, I.V. Timofeev. *Vestn. Novosib. Gos. Univ. Ser.: Fiz.*, **11** (4), 78 (2016) (in Russian). DOI: 10.54362/1818-7919-2016-11-4-78-104
- [13] A.V. Arzhannikov, S.L. Sinitskiy, D.A. Starostenko, P.V. Logachev, P.A. Bak, D.A. Nikiforov, S.S. Popov, P.V. Kalinin, D.A. Samtsov, E.S. Sandalov, M.G. Atlukhanov, A.N. Grigor'ev, S.O. Vorob'ev, D.V. Petrov, R.V. Protas. *Sib. Fiz. Zh.*, **18** (1), 28 (2023) (in Russian). DOI: 10.25205/2541-9447-2023-18-1-28-42
- [14] E.S. Sandalov, S.L. Sinitsky, A.V. Burdakov, P.A. Bak, K.I. Zhivankov, E.K. Kenzhebulatov, P.V. Logachev, D.I. Skovorodin, A.R. Akhmetov, O.A. Nikitin. *IEEE Transactions Plasma Sci.*, **49** (2), 718 (2021). DOI: 10.1109/TPS.2020.3045345
- [15] D.A. Nikiforov, A.V. Petrenko, S.L. Sinitsky, P.A. Bak, D.I. Skovorodin, P.V. Logachev, K.I. Zhivankov, E.S. Sandalov, O.I. Meshkov, A.V. Ivanov, V.V. Fuodorov, A.A. Starostenko, O.A. Pavlov, G.I. Kuznetsov, A.A. Krylov, D.A. Starostenko, O.A. Nikitin, A.R. Akhmetov. *J. Instrumentation*, **16** (11), P11024 (2021). DOI: 10.1088/1748-0221/16/11/P11024
- [16] A.V. Sidorov, A.P. Veselov, A.V. Vodopyanov, A.A. Murzanev, A.N. Stepanov. *Tech. Phys.*, **69** (7), 946 (2024). DOI: 10.61011/JTF.2024.07.58335.135-24
- [17] T. Tisovsky, T. Vit. *Europ. Phys. J. Conf.*, **2017-143**, 02131 (2017). DOI: 10.1051/epjconf/201714302131
- [18] V.V. Nikonov. *Izv. Samar. Nauchn. Tsentra Ross. Akad. Nauk*, **19** (1), 183 (2017).
- [19] W. Sutherland. *Philosoph. Magazine*, **36** (223), 507 (1893). DOI: 10.1080/14786449308620508
- [20] B.J. McBride, S. Gordon, M.A. Reno. *Coefficients for Calculating Thermodynamic and Transport Properties of Individual Species. NASA Technical Memorandum 4513* (NASA, 1993)
- [21] D.A. Samtsov, A.V. Arzhannikov, S.L. Sinitsky, E.S. Sandalov, M.A. Makarov, P.V. Kalinin, K.N. Kuklin. 8-th Intern. Conf. *Frontiers of Nonlinear Phys.*, **151**, 2024. <https://fnp2024.physconf.org/api/files/viii%20international%20conference-2024.pdf>

Translated by D.Safin